

Exact solution for quantum dynamics of a periodically-driven two-level-system

Anirban Gangopadhyay, Maxim Dzero, and Victor Galitski
*Condensed Matter Theory Center and Department of Physics,
University of Maryland, College Park, MD 20742-4111, U.S.A.*

We present a family of exact analytic solutions for non-linear quantum dynamics of a two-level system (TLS) subject to a periodic-in-time external field. In constructing the exactly solvable models, we use a “reverse engineering” approach where the form of external perturbation is chosen to preserve an integrability constraint, which yields a single non-linear differential equation for the ac-field. A solution to this equation is expressed in terms of Jacobi elliptic functions with three independent parameters that allows one to choose the frequency, average value, and amplitude of the time-dependent field at will. This form of the ac-drive is especially relevant to the problem of dynamics of TLS charge defects that cause dielectric losses in superconducting qubits. We apply our exact results to analyze non-linear dielectric response of such TLSs and show that the position of the resonance peak in the spectrum of the relevant correlation function is determined by the quantum-mechanical phase accumulated by the TLS wave-function over a time evolution cycle. It is shown that in the non-linear regime, this resonance frequency may be shifted strongly from the value predicted by the canonical TLS model. We also analyze the “spin” survival probability in the regime of strong external drive and recover a coherent destruction of tunneling phenomenon within our family of exact solutions, which manifests itself as a strong suppression of “spin-flip” processes and suggests that such non-linear dynamics in LC-resonators may lead to lower losses.

PACS numbers: 03.65.Yz, 42.50.Hz, 03.67.Lx

I. INTRODUCTION

The problem of a periodically-driven two-level system (TLS) appears in many physical contexts including magnetism, superconductivity, structural glasses and quantum information theory.¹⁻⁷ The interest in this old problem has been revived recently due to advances in the field of quantum computing (see, *e.g.*, Refs. [8–12] and references therein). First of all, a qubit itself is a two-level system and the question of its evolution under an external time-dependent perturbation is obviously of interest. Also, the physical mechanism that currently limits coherence particularly in superconducting qubits is believed to be due to other types of unwanted TLSs within the qubit, whose charge dynamics under a periodic-in-time electric field gives rise to dielectric losses directly probed in experiment.^{13,14} In what follows, we mostly apply our solution to the latter charge TLS model, but the general methods and some particular results of this work evidently can be applied to a much broader range of problems (see, *e.g.*, Ref. [15] and references therein).

One of the key metrics of a superconducting qubit is the quality factor, which is defined as a ratio of the real and imaginary parts of the dielectric response function, $\varepsilon(\omega)$, evaluated at the resonant frequency of the corresponding LC-circuit, $Q = \text{Re} \varepsilon(\omega_r) / \text{Im} \varepsilon(\omega_r)$. Very high values of the quality factor are required for the qubit to be operational. However, existing experiments consistently show significant dielectric losses that occur in an amorphous dielectric (*e.g.*, in Al_2O_3) used as a barrier in the Josephson junctions. It is believed that the losses are primarily due to the presence of charge two-level system defects in the barrier and/or the contact interfaces, which respond to an AC electric field in the LC-resonator. It

is still unclear what the physical origin of these defects is, but an early work of Phillips¹⁶ as well as very recent comprehensive density functional theory studies of Musgrave¹⁷ point to the OH-rotor defects as a very likely source of the dielectric loss. To determine the physical origin and the properties of the TLSs responsible for the dielectric loss is one of the central questions in the field of superconducting quantum computing and it has been largely the main physical motivation for our work.

The usual theoretical approach to calculating the quality factor and more generally the full dielectric response function, $\varepsilon(\omega)$, involves a formal mapping of charge dynamics in a double-well potential under the problem of “spin” dynamics in an AC field, described by the “spin” Hamiltonian $\hat{\mathcal{H}}(t) = \mathbf{b}(t) \cdot \hat{\sigma} / 2$, where $\hat{\sigma}$ denotes the Pauli matrices and $\mathbf{b}(t) = 2 \left(\Delta_t, 0, \varepsilon + \vec{d}_{\text{TLS}} \cdot \vec{E}(t) \right)$ is an effective “magnetic field” that drives TLSs, with ε , Δ_t , and \vec{d}_{TLS} being the TLS energy splitting, the tunneling amplitude between its two states, and the TLS dielectric moment correspondingly and $\vec{E}(t)$ is the AC electric field. A linear analysis within the canonical TLS model predicts that the dielectric function due to identical TLSs is peaked at the frequency, $\nu = \sqrt{\Delta_t^2 + \varepsilon^2}$. Ad-hoc inclusion of T_1 and T_2 relaxation processes and the assumption about random distribution of TLS energy-splittings and tunnelings (typically assumed to be uniform and log-uniform correspondingly) lead to the quality factor $Q \propto \sqrt{1 + (E_0/E_c)^x}$, with $x \sim 2$, E_0 being the amplitude of an applied AC electric field and E_c is a critical value of the amplitude which also encodes the information on the strength of the relaxation processes (see, *e.g.*, Ref. [5]). Both formulas are used widely in interpreting experimental data and probing energetics of the relevant

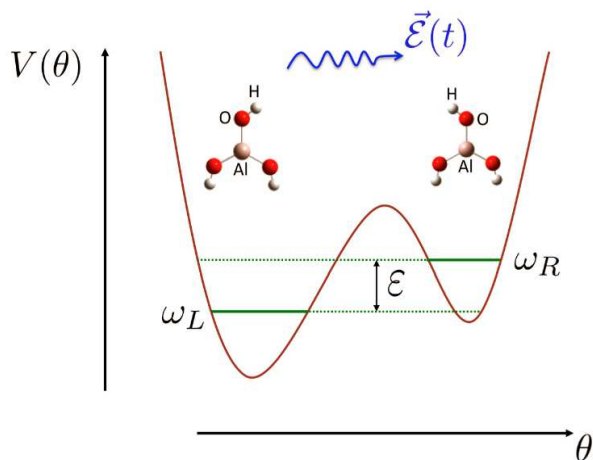


FIG. 1: Schematic representation of an OH-rotor two-level system in an Al_2O_3 oxide.^{16,17} Here, the role of the generalized variable is assigned to the angle θ defined as an angle between the OH-bond and an axis perpendicular to the vertical AlO bond. At low enough temperatures, the phase space an isolated rotor is reduced to the two-states corresponding to the minima of the double-well potential $V(\theta)$. Application of external ac-field parametrically coupled to the rotor's dipole moment induces oscillations between the two minima.

TLS defects^{5,13}. While this linear analysis is a fine approximation to describe a majority of regimes currently studied experimentally, the existing experiments are certainly capable and some do¹⁸ access non-linear regimes as well, where the energy of the applied electric field is comparable or larger than the relevant TLS energies. Hence, this non-perturbative regime is of clear experimental and theoretical interest. More importantly studies of non-linear dynamics may provide another effective means to probe the properties of TLSs.

The mathematical formulation of the non-linear TLS dynamics problem studied in this paper is deceptively simple: We wish to solve the Schrödinger equation for a spinor wave-function, $\Psi = \begin{pmatrix} \psi_+ \\ \psi_- \end{pmatrix}$, $i\partial_t \Psi = \frac{1}{2} \mathbf{b}(t) \cdot \hat{\sigma} \Psi$ that describes a half-integer spin subject to a periodic-in-time magnetic field of the form, $\mathbf{b}(t) = 2(\Delta_t, 0, f(t))$, where Δ_t is a constant describing the coupling between the two states and the function $f(t) = f(t+T)$ describes the time dependent perturbation. Despite the simplicity of the formulation, the problem is generally unsolvable in analytic form for most cases of practical interest. The origin of this surprising fact can be understood if we introduce a new function $R(t) = \psi_+(t)/\psi_-(t)$, which reduces the matrix Schrödinger equation to the Riccati equation $\partial_{(-it)} R = 2fR + \Delta_t [1 - R^2]$. It is a non-linear differential equation that has known analytic solution in a very limited number of cases (note that the case of a monochromatic perturbation is not one of them). Therefore, to solve for TLS dynamics driven by a specific non-equilibrium field is equivalent to generating a particular solution to the Riccati equation corresponding to this

perturbation. Clearly this is a challenging mathematical task and this observation partially explains the current deficit of exact mathematical results. The difficulties in obtaining exact solutions have led to the emergence of several perturbative approaches, used in particular to characterize relaxation and dephasing rates in qubits as a function of driving amplitude (see, *e.g.*, Ref. [15] and references therein). These analyses provide very useful physical insights and correctly describe the physics if the time-dependent perturbation is weak, but it is also clear that there exist non-linear effects beyond perturbation theory and it is desirable to have exact results to access this qualitatively different physics.

The mathematical approach that we use in this paper to obtain exact results is to “reverse engineer” exactly solvable Hamiltonians of specific form relevant to the problem of interest. A key observation in our analysis is that finding a Hamiltonian corresponding to a given solution is much easier than solving the Schrödinger equation with a given Hamiltonian. In some generalized sense, the two procedures are related to one another much like differentiation relates to integration. To see this, it is useful to consider the evolution operator, or the \hat{S} -matrix, which relates the initial state at $t = 0$ to a final state at $t > 0$ as follows, $\Psi(t) = \hat{S}(t)\Psi(0)$. In the absence of relaxation process the time-evolution is unitary and it satisfies the Schrödinger equation, $i\partial_t \hat{S}(t) = \hat{\mathcal{H}}(t)\hat{S}(t)$. If we choose an arbitrary S-matrix, $\hat{S} = \exp[-\frac{i}{2}\Phi(t) \cdot \hat{\sigma}] \in SU(2)_2$, we can immediately reconstruct the corresponding Hamiltonian that gives rise to such evolution as follows $\hat{\mathcal{H}}(t) = i\partial_t \hat{S}(t)\hat{S}^\dagger(t)$. Using this method, one can generate an infinite number of exact non-equilibrium solutions and explicit models. These solutions may be of importance to physics of NMR, to the question of physical implementation of gate operations on a qubit as well as of some mathematical interest. Nevertheless without additional constraints such analyses would generally produce Hamiltonians of little importance to the problem of dynamics of TLS charge defects.

A very useful insight that allows us to constructively narrow down the range of relevant dynamical systems comes from the mathematically related problem of far-from-equilibrium superconductivity¹⁹⁻²¹. It is well-known that the reduced BCS Hamiltonian is algebraically equivalent to an interacting XY-spin model in an effective “inhomogeneous” magnetic field in the z -direction, whose profile is dictated by the bare single particle-energy dispersion. Far from equilibrium, dynamics of a given Anderson pseudospin²² is determined by an effective time-dependent self-consistent field of other pseudo-spins that it interacts with.²³ In many cases (determined by specific initial conditions), this BCS self-consistency constraint dynamically selects a specific order-parameter, such that the dynamics of essentially infinite number of spins is equivalent to the dynamics of few spins only.²¹ For special sets of initial conditions, these spins move in unison and therefore the self-consistent “magnetic field” (or superconducting order parameter in the language of BCS the-

ory) is periodic in time. The reduced BCS model is integrable and there exists a very elegant prescription for constructing exact non-equilibrium solutions to it, developed primarily by Yuzbashyan and collaborators.^{20,21,24} These solutions contain, in particular, exact spin dynamics in a periodic time-dependent field that can be expressed in terms of elliptic functions. In this paper, we generalize such anomalous soliton solutions of Yuzbashyan²⁵ to encompass a wider range of time dependencies relevant to the problem of TLS dynamics, which is of our primary interest.

This paper is organized as follows: Sec. II summarizes a general mathematical structure behind the “reverse engineering” approach to constructing exact solutions for non-linear TLS dynamics. The specific Ansatz and technical details of our particular family of solutions for periodically-driven TLS dynamics are given in Sec. III. In Sec. IV, we use some representative solutions to illustrate the emergence of the coherent destruction of tunneling phenomenon. We also derive the spectrum of exact dielectric response function due to an ensemble of identical charge TLS in the presence of dissipation, which is introduced phenomenologically. In Sec. V we provide a summary of our results. In the Appendices we list some technical details of our calculations as well as useful relations aimed to shed more light on the subtle features of our theory.

II. GENERAL FRAMEWORK FOR CONSTRUCTING EXACT SOLUTIONS

In this paper, we derive a family of exact solutions for the non-dissipative TLS dynamics subject to an external ac-field. The main ingredient of our approach is a special Ansatz for the TLS’s dynamics that corresponds to periodic-in-time but non-monochromatic external fields. Before proceeding to the specific Ansatz, let us first introduce a general algebraic framework for “reverse engineering” of exact solutions. We are interested in solving the non-equilibrium Schrödinger equation for the spinor $\Psi(t)$

$$i\partial_t\Psi(t) = \hat{\mathcal{H}}(t)\Psi(t), \quad \Psi(t) = \begin{pmatrix} \psi_+ \\ \psi_- \end{pmatrix}. \quad (1)$$

where the Hamiltonian is $\hat{\mathcal{H}}(t) = \frac{1}{2}\mathbf{b}(t)\cdot\hat{\boldsymbol{\sigma}}$. As mentioned in the introduction, instead of solving Eq. (1) for the wave-function, we can consider the Schrödinger equation for the evolution operator that relates the initial and final states, $\Psi(t) = \hat{S}(t)\Psi(0)$. This equation for the S -matrix has the form identical to Eq. (1):

$$i\partial_t\hat{S}(t) = \hat{\mathcal{H}}(t)\hat{S}(t), \quad \text{and} \quad \hat{S}(0) = \hat{1} \quad (2)$$

but now it is an equation for the matrix function $\hat{S}(t)$, which belongs to the two-dimensional representation of the $SU(2)$ group, while the Hamiltonian expressed in terms of $SU(2)_2$ generators belongs to the two-dimensional representation of the $su(2)$ algebra. Note

that the form of Eq. (2) is such that it may be generalized to an arbitrary spin or equivalently to an arbitrary-dimensional representation of $SU(2)$ or it can be viewed as an equation of motion in the abstract group such that $\hat{\mathcal{H}}_{\text{abs}}(t) = \mathbf{b}(t) \cdot \hat{\mathbf{J}}_{\text{abs}} \in su(2)$ and $\hat{S}_{\text{abs}}(t) = \exp\left[-i\boldsymbol{\Phi}(t) \cdot \hat{\mathbf{J}}_{\text{abs}}\right] \in SU(2)$, where $\hat{\mathbf{J}}_{\text{abs}}$ are the corresponding generators. Therefore, a solution of the problem in a particular representation, *i.e.*, an explicit form of $\boldsymbol{\Phi}(t)$, immediately gives the corresponding solutions in all other representations (*e.g.*, a two-level-system dynamics uniquely determines a “ d -level system” dynamics in the same field). This TLS problem that we are interested in corresponds to the two-dimensional generators $\hat{J}_\alpha^{(2)} = \frac{1}{2}\hat{\sigma}_\alpha$ with $\hat{\sigma}_\alpha$ ($\alpha = x, y, z$) being the familiar Pauli matrices.

The problem of determining the solution, $\boldsymbol{\Phi}(t)$, from the magnetic field time-dependence $\mathbf{b}(t)$ is a complicated one, but the inverse problem is almost trivial. Indeed, if we select a specific S -matrix (defined uniquely by the choice of a specific function, $\boldsymbol{\Phi}(t)$), the Hamiltonian will read

$$\hat{\mathcal{H}}(t) = i\partial_t\hat{S}(t)\hat{S}^\dagger(t), \quad (3)$$

where

$$\hat{S}(t) = \exp\left[-\frac{i}{2}\boldsymbol{\Phi}(t) \cdot \hat{\boldsymbol{\sigma}}\right]. \quad (4)$$

Using the algebraic identities for the Pauli matrices, we obtain the corresponding magnetic field

$$\mathbf{b}(t) = \dot{\Phi} \mathbf{n} + \sin \Phi \dot{\mathbf{n}} + (1 - \cos \Phi) [\mathbf{n} \times \dot{\mathbf{n}}], \quad (5)$$

where $\boldsymbol{\Phi}(t) = \Phi(t)\mathbf{n}(t)$, with $|\mathbf{n}(t)| \equiv 1$. Note that one can generate exactly-solvable models by simply picking an arbitrary $\boldsymbol{\Phi}(t)$ dependence and using Eq. (3) to find the corresponding Hamiltonian. However, without guidance or luck, such an analysis would generally produce complicated non-equilibrium fields that have little to do with an underlying physical problem. Let us however mention here that this procedure may be of interest to quantum computing in general, because the time-evolution governed by an S -matrix can be viewed as a “gate operation” on the spin (if the TLS/spin corresponds to a qubit rather than to a defect within a qubit). By picking “trajectories,” $\boldsymbol{\Phi}(t)$, on the algebra that start in the origin, *i.e.* $\boldsymbol{\Phi}(0) = \mathbf{0}$, but end at a specific point at a time T , one can immediately determine the non-equilibrium magnetic pulse, $\mathbf{b}(t)$, or a class of such pulses, that will give rise to a desired gate operator $\hat{G} \equiv \hat{S}(T) = \exp\left[-\frac{i}{2}\boldsymbol{\Phi}(T) \cdot \hat{\boldsymbol{\sigma}}\right]$.

Let us note here that the function, $\boldsymbol{\Phi}(t)$, contains complete information about the solution to the original problem, Eq. (1), including the overall quantum phase accumulated by the wave-function during the time evolution (as we shall see below, this phase is of particular interest to the problem of dielectric response of TLSs in superconducting qubits). An interesting question is whether

and how this purely quantum phase can be restored from a solution of the corresponding classical Bloch equations that are usually considered in this context. Let us recall that a classical mapping can be achieved by introducing the average magnetic moment,

$$\mathbf{m}(t) = \Psi^\dagger(t) \frac{\hat{\boldsymbol{\sigma}}}{2} \Psi(t). \quad (6)$$

Therefore, $\mathbf{m}^2(t) \equiv 1/4$ and the classical equations of motion for the spin moment follow from $\partial_t \mathbf{m}(t) = \frac{1}{2} \Psi^\dagger(t) [\hat{\mathcal{H}}(t), \hat{\boldsymbol{\sigma}}] \Psi(t)$ and yield the familiar result

$$\partial_t \mathbf{m}(t) = \mathbf{b}(t) \times \mathbf{m}(t). \quad (7)$$

Let us recall that these Bloch equations are a saddle point of quantum spin dynamics, much in the same way that Newton's equations of motion governed by the force, $[-\nabla V(\mathbf{r})]$, represent a saddle point of the action describing a quantum particle in the potential, $V(\mathbf{r})$, and therefore do not contain direct information about quantum interference and tunneling effects. Similarly, Eqs. (7) do not directly contain the quantum phase and to determine it one has to go back to the Schrödinger equation. Another more abstract way to see this is by noticing that Eqs. (7) describe the motion on a two-dimensional (Bloch) sphere, $\mathbf{m}(t) \in S^2$, while the original quantum problem Eq. (2) describes motion on a three-dimensional sphere since $\hat{S}_{\text{abs}}(t) \in SU(2) \sim S^3$. Now let us recall that there exists the Hopf fibration such that $SU(2)/U(1) = S^2$, which summarizes the fact that classical equations, namely Eqs. (7), represent quantum motion modulo the $U(1)$ phase dynamics. Fortunately, this phase dynamics can generally be restored from exact dependence of the $\mathbf{m}(t)$ solution, albeit in a non-local way. To see this, we can write the magnetization in terms of the S -matrix as follows $\mathbf{m}(t) = \frac{1}{2} \Psi^\dagger(0) [\hat{S}^\dagger(t) \hat{\boldsymbol{\sigma}} \hat{S}(t)] \Psi(0)$, where $\Psi(0)$ and the corresponding $\mathbf{m}(0) = \Psi^\dagger(0) \frac{\hat{\boldsymbol{\sigma}}}{2} \Psi(0)$ are initial conditions for the wave-function and Bloch magnetization, correspondingly. Using again the well-known identities for the Pauli matrices, we find the evolution matrix for the Bloch equations, $m_\alpha(t) = R_{\alpha\beta}(t) m_\beta(0)$, as follows

$$R_{\alpha\beta}(t) = \delta_{\alpha\beta} \cos \Phi + n_\alpha n_\beta (1 - \cos \Phi) - \varepsilon_{\alpha\beta\gamma} n_\gamma \sin \Phi. \quad (8)$$

This three-dimensional matrix describes a rotation, $\hat{R}(t) \in SO(3)$, and can be represented equivalently as

$$\hat{R}(t) = \exp \left[-\Phi(t) \cdot \hat{\mathbf{L}} \right], \quad \text{where } \hat{\mathbf{L}} = \begin{pmatrix} 0 & -\mathbf{e}_z & \mathbf{e}_y \\ \mathbf{e}_z & 0 & -\mathbf{e}_x \\ -\mathbf{e}_y & \mathbf{e}_x & 0 \end{pmatrix}, \quad (9)$$

where $\hat{\mathbf{L}} \in so(3) \sim su(2)$ belong to the three-dimensional vector representation of the $su(2)$ algebra. They are related to the "usual" spin-1 representation (where $\hat{J}_z^{(3)}$ is diagonal) via a simple linear transform.

Therefore, we see that if we know an arbitrary solution to the Bloch equations, $\mathbf{m}(t)$ we can at least in

principle restore the function, $\Phi(t)$, [see, Eqs. (9) and (4)], which uniquely determines the entire quantum solution. It also suggests that if we choose an arbitrary dynamic function on a sphere we may be able to restore the quantum Hamiltonian that would give rise to it, via mappings $\mathbf{m}(t) \rightarrow \hat{R}(t) \rightarrow \Phi(t) \rightarrow \hat{S}(t) \rightarrow \hat{\mathcal{H}}$. However, the second step in this chain of transforms involves effectively calculating a logarithm of the rotation matrix, which due to a complicated "analytic" structure of this matrix-logarithm function requires a careful calculation non-local in time.

The subsequent Sections are devoted to constructing exactly solvable periodic-in-time Hamiltonians based on a specific Ansatz for the classical Bloch "magnetization," $\mathbf{m}(t)$. It further involves a restoration of the corresponding quantum $U(1)$ phase via a straightforward integration. More specifically, we "reverse engineer" the following Hamiltonian

$$\hat{\mathcal{H}} = \Delta_t \hat{\sigma}_x + f(t) \hat{\sigma}_z. \quad (10)$$

where $f(t) = f(t + T_f)$ is a periodic function, with an arbitrary period, T_f . Our solution below also allows tuning of the average splitting, $\varepsilon = \langle f(t) \rangle_{T_f}$, and the AC

field amplitude, $A_f \sim \sqrt{\langle [f(t) - \varepsilon]^2 \rangle_T}$. As mentioned in the introduction, this problem is of great importance to the physical problem of externally-driven TLS dynamics in superconducting qubits (with Δ_t corresponding to tunneling between the wells, ε to a splitting of energy levels in a double-well potential, and T_f and A_f being the period and the amplitude of the AC-electric field correspondingly).

Our "guess" for the relevant Ansatz for the Bloch "magnetization," $\mathbf{m}(t)$, is based on a set of formal solutions discovered in the related problem of quenched dynamics of fermionic superfluids.^{19-21,24,25} Formally, the quenched dynamics of each individual Cooper pair is described by the Bogoliubov-de Gennes Hamiltonian, which is essentially a spin Hamiltonian that reduces to (10) after the unitary transformation $\hat{\sigma}_x \rightarrow \hat{\sigma}_z$ and $\hat{\sigma}_z \rightarrow -\hat{\sigma}_x$, with Δ_t corresponding to a single particle energy level and $f(t)$ to the superfluid order parameter. A realization of each particular form of the superfluid order parameter dynamics in a steady state can be unambiguously determined by the initial conditions²¹ using the exact integrability of BCS model.²⁰ Note that a self-consistency condition for the order parameter provides a limitation on the set of functions for which the corresponding problem is integrable and for some initial conditions periodic-in-time self-consistent dynamics, $f(t)$, can be realized. While in our TLS problem, there is no natural self-consistency constraint, such insights and constraints from the BCS problem help us narrow down the range of possible Ansatzes to restore reasonable physical Hamiltonians, which are also exactly solvable by construction.

In what follows, we generalize the soliton analysis of Yuzbashyan²⁵ and find a general soliton configuration, characterized by three independent parameters, which

we denote as Δ_{\pm} and Δ_a . For the physical problem of interest, this conveniently implies that some, generally speaking, non-trivial combination of these parameters will determine the arbitrary frequency, amplitude, and the dc-component of the field. Due to the periodicity, we can generally represent the AC-perturbation as a Fourier series

$$f(t) = \varepsilon + \mathcal{A}_f \sum_{n=1}^{\infty} \tilde{f}_n \cos(n\omega_f t). \quad (11)$$

Note that for certain specific choices of the parameters $\Delta_{\pm, a}$, the leading coefficient $\tilde{f}_1 \gg \tilde{f}_n$ ($n = 2, 3, \dots$) and one recovers the limit of a monochromatic AC-field, albeit in the regime of weak driving ($\mathcal{A}_f \tilde{f}_1 \ll \max\{\Delta_t, \varepsilon\}$). Therefore, our non-linear analysis contains the standard linear response results as a simple special case.

III. NON-DISSIPATIVE DYNAMICS OF THE AC-DRIVEN TLS

In this Section we provide the details on the derivation of the exact solution for the TLS dynamics. We devote the special attention to the analysis of the U(1) phase of the wave function. We also elucidate the relations between the parameters of our solution and the amplitude, phase and the dc-component of the external field, which may be useful for experimental applications of our theory.

A. Ansatz

We now focus on the Schrödinger equation for the half-integer spin in the magnetic field, $\mathbf{b}(t) = 2(\Delta_t, 0, f(t))$. When written in terms of spinor components, it has the form

$$\begin{cases} i\dot{\psi}_+ = \Delta_t \psi_- + f(t)\psi_+ \\ i\dot{\psi}_- = \Delta_t \psi_+ - f(t)\psi_- \end{cases}. \quad (12)$$

The corresponding Bloch equation is

$$\dot{\mathbf{m}}(t) = 2(\Delta_t, 0, f(t)) \times \mathbf{m}(t). \quad (13)$$

Let us now make the following Ansatz for its exact solution:²⁵

$$m_x = D - C f^2, \quad m_y = B \dot{f}, \quad m_z = A f(t) + F. \quad (14)$$

From two of the Eqs. (13) we find $A = 2\Delta_t B$ and $B = C$. Thus among five parameters in (14) only three are independent: F, B and D . The equation for the external field, $f(t)$, can be obtained from (14) using the condition $\mathbf{m}^2 = 1/4$. This resulting equation for the function $f(t)$ acquires the form

$$\dot{f}^2 = -f^4 - 4c_2 f^2 + 8c_1 f - 4c_3, \quad (15)$$

where coefficients c_j are given by some combinations of parameters B, D and F [see Eqs. (30) below]. Equation

(15) can be cast to a more symmetric form, using another set of parameters Δ_a and Δ_{\pm} , which are chosen to be positive and are related to coefficients c_j as follows:

$$\begin{aligned} c_1 &= -\frac{\Delta_a}{4}(\Delta_+^2 - \Delta_-^2), \\ c_2 &= -\frac{1}{4}(\Delta_+^2 + \Delta_-^2 + 2\Delta_a^2), \\ c_3 &= -\frac{1}{4}(\Delta_+^2 - \Delta_a^2)(\Delta_a^2 - \Delta_-^2). \end{aligned} \quad (16)$$

Without loss of generality and to be more specific we also assume $\Delta_+ \geq \Delta_-$ for the remainder of this paper, while Δ_a can be assigned an arbitrary value. By virtue of expressions (16) equation (15) now reads

$$\dot{f}^2 = [(f - \Delta_a)^2 - \Delta_-^2][\Delta_+^2 - (f + \Delta_a)^2]. \quad (17)$$

Below we will make several transformations that allow us to reduce (17) to an equation for the Weierstrass elliptic function.²⁶ Firstly, let us introduce a function, $y(t)$,

$$f(t) = \Delta_+ \left[\frac{2}{y(t)} - 1 \right] - \Delta_a \quad (18)$$

which satisfies the following equation

$$\left(\frac{dy}{dx} \right)^2 = 4(y - a_+)(y - a_-)(y - 1), \quad x = \frac{\Delta_+ t}{\sqrt{a_+ a_-}}, \quad (19)$$

where $a_{\pm} = 2\Delta_+ / (\Delta_+ + 2\Delta_a \pm \Delta_-)$. Now, Eq. (19) can be easily reduced to a well-known equation for the Weierstrass elliptic function by rescaling the parameters via the transformation

$$y(x) = Z(x) + \frac{a_+ + a_- + 1}{3}, \quad (20)$$

so that

$$\left(\frac{dZ}{dx} \right)^2 = 4(Z - e_1)(Z - e_2)(Z - e_3), \quad (21)$$

where parameters e_j satisfy the following conditions $e_1 > e_2 > e_3$ and $e_1 + e_2 + e_3 = 0$. Coefficients e_j are determined by the parameters Δ_a and Δ_{\pm} . The specific expressions for the coefficients e_j , however, depend on the relative values of the initially introduced set of parameters and are given in Appendix A. Solution of the equation (21) is

$$Z(x) = \mathcal{P}(x + \omega'), \quad \omega' = \frac{\mathbf{K}(\kappa')}{\sqrt{e_1 - e_3}}, \quad (22)$$

where $\mathcal{P}(x)$ is a Weierstrass elliptic function, \mathbf{K} is a complete elliptic integral of the first kind²⁶ and $\kappa' = \sqrt{(e_1 - e_2)/(e_1 - e_3)}$. Function $Z(x)$ is a doubly-periodic function with the period along the physical time axis determined by, $l = 2\omega$, where $\omega = \mathbf{K}(\kappa)/\sqrt{e_1 - e_3}$ and $\kappa = \sqrt{1 - \kappa'^2}$ is a modulus of elliptic functions. Combining (22) with Eqs. (20) and (18) allows us to express

$f(t)$ in terms of elliptic functions. Expression for $f(t)$ can be compactly written in terms of Jacobi elliptic functions. Just as it is the case for the parameters e_j , the particular form of the resulting expression depends on the relation between Δ_a and Δ_{\pm} (see Appendix A).

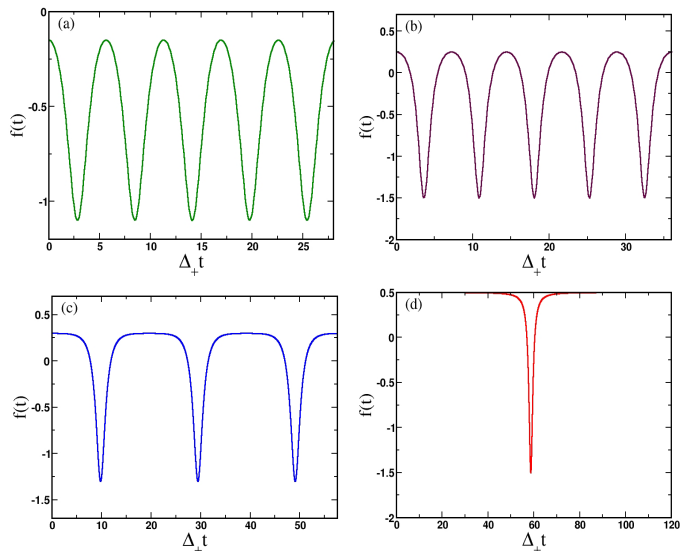


FIG. 2: Plots of the function $f(t)$ (23) in units of Δ_+ for different values Δ_a : (a) $\Delta_a = 0.1\Delta_+$, $\Delta_- = 0.3\Delta_+$; (b) $\Delta_a = 0.5\Delta_+$, $\Delta_- = 0.3\Delta_+$; (c) $\Delta_a = 0.3\Delta_+$, $\Delta_- = 0.1\Delta_+$; (d) $\Delta_a = 0.5\Delta_+$, $\Delta_- = 0.001\Delta_+$. We note that for the choice of the parameters (d) the period of $f(t)$ diverges. The curves above are plotted for the value of $\Delta_t = 0.5\Delta_+$.

All cases considered here are summarized by the following compact expression for the function, $f(t)$, written in terms of Jacobi elliptic function sn as follows:

$$f(t) = \Delta_+ \frac{\eta_+ \text{sn}^2(z, \kappa) - 1}{\eta_- \text{sn}^2(z, \kappa) + 1} - \Delta_a, \quad (23)$$

where variable z is

$$z = \frac{(t - t_0)}{2} \sqrt{[(\Delta_+ + 2\Delta_a)^2 - \Delta_-^2] (e_1 - e_3)} \quad (24)$$

and $t_0 = -\omega' \sqrt{a_+ a_-} / \Delta_+$. If we consider Δ_{\pm} fixed, then the parameters η_{\pm} are given by one of the following expressions depending on the value of Δ_a :

$$\eta_{\pm} = \begin{cases} \frac{1}{e_1 - e_3} \pm 1, & \Delta_a > \frac{\Delta_+ + \Delta_-}{2} \\ \frac{1}{e_1 - e_3} \pm \kappa^2, & \frac{\Delta_+ - \Delta_-}{2} \leq \Delta_a \leq \frac{\Delta_+ + \Delta_-}{2} \\ \frac{1}{e_1 - e_3}, & \Delta_a < \frac{\Delta_+ - \Delta_-}{2} \end{cases}. \quad (25)$$

Fig. 2 displays some representative dependencies of the driving field from the class of solutions described by Eqs. (23), (24), and (25). Note that the curve in Fig. 2a is visually indistinguishable from a harmonic periodic signal, Fig. 1b and Fig. 1c contain apparent non-monochromatic contributions to the periodic signal, and finally Fig. 2d provides an example of a degenerate case,

or a single soliton, where the period of the elliptic function is taken to be infinite. Fig. 3 shows dynamic trajectories of the ‘‘magnetization’’ on the Bloch sphere given by exact Eq. (14) that correspond to these particular $f(t)$ -dependencies.

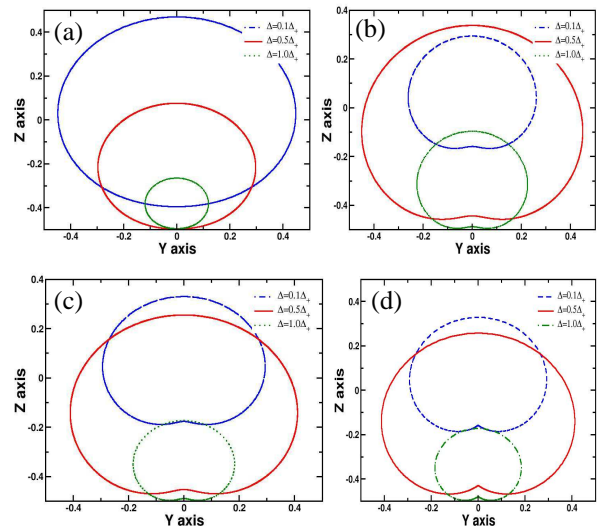


FIG. 3: TLS dynamics on the Bloch sphere (13,14). Trajectories of TLS for the solutions described by Eq. (23) and depicted in Fig. 2 for the various set of parameters Δ_a and Δ_{\pm} . The latter take the same values used on Fig. 2.

From the expression for the external field (23) it is, however, not immediately clear what set of parameters correspond to the regimes of weak and strong ac-driving. To clarify this issue, let us re-write (23) in the form more useful for practical applications. Let us first explicitly derive the amplitude, frequency and the dc-component of function $f(t)$. The period and the amplitude of oscillations of $f(t)$ can be immediately deduced from (23,24):

$$T_f = \frac{4\mathbf{K}(\kappa)}{\sqrt{[(\Delta_+ + 2\Delta_a)^2 - \Delta_-^2] (e_1 - e_3)}}, \quad (26)$$

$$\mathcal{A}_f = \frac{\Delta_+}{2} \left(\frac{\eta_+ + \eta_-}{\eta_- + 1} \right).$$

Lastly, the average value of the function $f(t)$ over its period is

$$\langle f(t) \rangle = \frac{\Delta_+ \eta_+}{\eta_-} \left[1 - \frac{(\eta_+ + \eta_-)}{\eta_+ \mathbf{K}(\kappa)} \Pi(-\eta_-, \kappa) \right] - \Delta_a \equiv \varepsilon, \quad (27)$$

with $\mathbf{K}(\kappa)$ and $\Pi(n, \kappa)$ being an complete elliptic integral of the first and third kind correspondingly. As we have already mentioned, quantity (27) describes the dc-component of the external field. One can view Eqs. (26, 27) as the definition of yet another set of parameters \mathcal{A}_f , $\omega_f = 2\pi/T_f$ and $\varepsilon = \langle f(t) \rangle$, which allows us to cast external field $f(t)$ into the form given by (11). We plot the

dependence of these parameters on the ratio Δ_-/Δ_+ in Fig. 4 for different values of Δ_a while keeping the value of Δ_t fixed. As we can see from 4 the limits of strong and weak ac-driving are easily attainable with the frame of our solution. In particular, we see that the regime of the strong ac-driving should be achieved for moderate values of Δ_a and $\Delta_-/\Delta_+ \sim 0.2$.

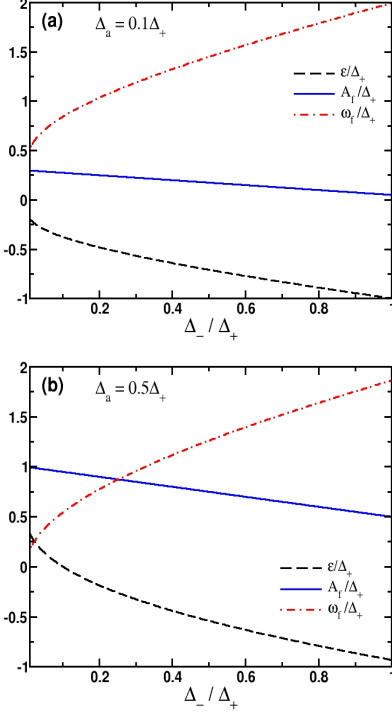


FIG. 4: Plots of the amplitude \mathcal{A}_f , frequency ω_f and dc-component ε of the external field $f(t)$, Eq. (11): (a) $\Delta_a = 0.1\Delta_+$, $\Delta_t = 0.3\Delta_+$; (b) $\Delta_a = 0.5\Delta_+$, $\Delta_t = 0.3\Delta_+$.

Expressions (23,24,25) constitute one of the main technical results of this paper. To get a further insight into the properties of our solution we refer the reader to Appendix B where we consider few limiting cases for the function (23). Quite generally, our solution represents the superposition of monochromatic waves with frequencies integer multiples of $\omega_f = 2\pi/T_f$. As discussed in the Appendix B, solution (23) can be reduced to the monochromatic wave with frequency $2\Delta_+$ when $\Delta_a = 0$ and $\Delta_- \simeq \Delta_+$.

B. Wave function

Having determined the form of the periodic field $f(t)$ we employ the relations (6) to compute the amplitudes $\psi_+(t)$ and $\psi_-(t)$. First let us represent these functions as follows²⁴

$$\psi_{\pm}(t) = |\psi_{\pm}(t)|e^{\mp i\phi(t)}e^{i\alpha(t)}. \quad (28)$$

From these expressions, it follows that absolute values of the components ψ_+ and ψ_- as well as their relative phase $\phi(t)$ are determined by the instantaneous value of magnetization (14). From Eqs. (6,14), we find

$$|\psi_{\pm}(t)| = \sqrt{\frac{1}{2} \pm 2\Delta_t B f(t) \pm F}, \quad (29)$$

$$\tan[2\phi(t)] = \frac{\dot{f}}{(D/B) - f^2(t)},$$

where parameters B and D are determined from

$$\frac{D}{B} = 2(\Delta_t^2 - c_2), \quad B = \frac{1}{4\sqrt{(\Delta_t^2 - c_2)^2 + \frac{c_1^2}{\Delta_t^2} - c_3}}, \quad (30)$$

$$F = -2c_1 B / \Delta_t.$$

and parameters c_j 's are given by (16). Note that apparent ambiguity in signs for the parameters B and D as well as for parameter F is resolved by fulfilling the condition $m^2 = 1/4$.

C. Restoring the U(1) phase

It has been mentioned above that the common phase $\alpha(t)$ has to be determined from the solution of the equations (12). At first sight the resulting equation for $\alpha(t)$ appears to be very complicated, but it can be significantly simplified using Eqs. (29), so that

$$\dot{\alpha} = -\frac{1}{2} \frac{f(t)m_z(t)}{[1/4 - m_x^2(t)]}. \quad (31)$$

After some algebraic manipulations, we find

$$\alpha(t) = \int_0^t \left\{ \Delta_t \left[\frac{d_+^2}{f^2(t') - d_+^2} - \frac{d_-^2}{f^2(t') - d_-^2} \right] + \frac{F}{2B^2} \frac{f(t')}{[f^2(t') - d_+^2][f^2(t') - d_-^2]} \right\} dt' + \alpha_0, \quad (32)$$

where α_0 is determined by the initial conditions, $d_{\pm}^2 = (1/2B) \pm D/B$. One can evaluate the integral in (32) exactly and express in terms of elliptic σ and ζ functions (see Appendix C for details of this calculation). We note that on the grounds of Floquet theory we can represent an expression for the phase $\alpha(t)$ as a sum of two terms:

$$\alpha(t) - \alpha_0 = -\nu t + \gamma(t), \quad (33)$$

where $\gamma(t) = \gamma(t + T_f)$ is a periodic function and ν is a constant. Analytic expression for both of these quantities can be extracted from the analytic expression for $\alpha(t)$ listed in Appendix C. For example, from (33) it follows $\nu = [\alpha(t) - \alpha(t + T_f)]/T_f$. In the limit when $\Delta_a = 0$ and $\Delta_- = \Delta_+$ we find $\nu = (\Delta_t^2 + \Delta_+^2)^{1/2}$, while in the limit when $\Delta_a = 0$ and $\Delta_- = 0$ we obtain $\nu =$

Δ_t . For a general set of values Δ_a and Δ_{\pm} the resulting expression for ν is not as simple as those listed above. For practical purposes, however, one can construct an approximate expression for ν . By analyzing the behavior of $\alpha(t)$ numerically we find that for $\Delta_a = 0$, frequency ν can be approximated (see Fig. 5a) by:

$$\nu(\Delta_a = 0) \approx \frac{1}{T_f} \int_0^{T_f} \sqrt{\Delta_t^2 + f^2(t)} dt. \quad (34)$$

We find qualitatively different behavior of ν as a function of $\delta = \Delta_-/\Delta_+$ for nonzero Δ_a . In that case, there appears to be a discontinuity in ν at some critical value of Δ_-/Δ_+ . The source of this discontinuity at least for small Δ_a lies in the fact that $\dot{\alpha}(t) \propto m_z(t)$ changes sign during its time evolution. For non-zero Δ_a there are always exists δ_c such that $m_z(t=0) = 0$, while for $\delta > \delta_c$ one observes $m_z(0 < t_{1,2} < T_f) = 0$. The sign change in $m_z(t)$ implies that the derivative of the quantum phase will change sign also (31), so that the subsequent integration yields the value of ν smaller than the one found for $\delta < \delta_c$, Fig. 5b.

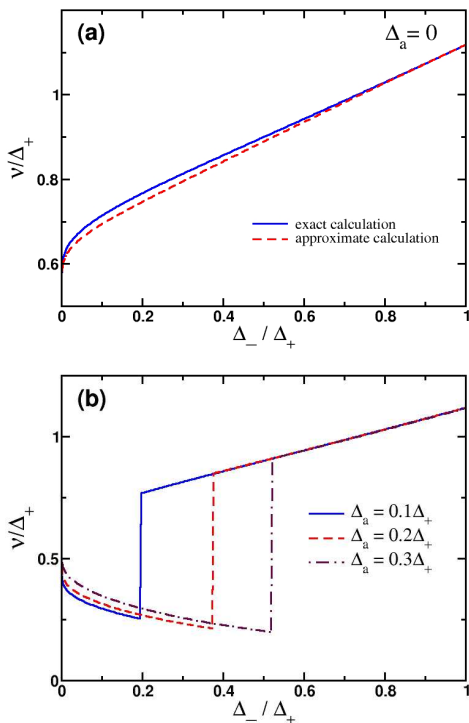


FIG. 5: Dependence of exponent ν as a function of the ratio Δ_-/Δ_+ for various values of Δ_a . On panel (a) we compare the result of numerical computation of ν from (32) and compare them with approximate expression (34) when $\Delta_a = 0$. Panel (b) shows the dependence of ν for $\Delta_a \neq 0$.

In order to get further insight into the physical meaning of the quantity ν , we can employ the analogy between the TLS and spin-1/2 and define the magnetization

$M_\alpha(t) = \langle \Psi_g(t) | \hat{\sigma}_\alpha | \Psi_g(t) \rangle / 2$, where $\Psi_g(t)$ is a general solution of the Schrödinger equation and can be expressed as a linear combination of the particular solution $\Psi(t)$ (see below). Then one can show²⁴ that the dynamics of the vector \vec{M} can be represented as a linear superposition of vector $\vec{m}(t)$ precessing with the frequency of the field $f(t)$ and a vector $\vec{h}(t)$ such that $\vec{h} \cdot \vec{m} = 0$. Each component of the latter oscillates with frequency ν . Our results from Fig. 3b suggest that the rate of precession of vector \vec{h} will be significantly reduced as one tunes the parameter Δ_-/Δ_+ .

The solution of the Schrödinger equation we described above is only a particular solution from which the general solution can be constructed straightforwardly by taking advantage of the underlying symmetries of Eqs. (12). A general solution for the wave function, $\Psi^\dagger = (\psi_+^*, \psi_-^*)$, can be presented as

$$\Psi_g(t) = C_1 \begin{pmatrix} \psi_+(t) \\ \psi_-(t) \end{pmatrix} + C_2 \begin{pmatrix} \psi_+^*(t) \\ -\psi_+^*(t) \end{pmatrix}, \quad (35)$$

where $C_{1,2}$ are integration constants, which satisfy $|C_1|^2 + |C_2|^2 = 1$ and are to be determined from the initial conditions. For example, for the specific choice of an initial condition when the TLS at $t = 0$ resides in one of its two states,

$$\Psi_g(0) = \begin{pmatrix} 1 \\ 0 \end{pmatrix}, \quad (36)$$

the coefficients $C_{1,2}$ are

$$C_1 = \psi_+^*(0), \quad C_2 = \psi_-(0). \quad (37)$$

Expressions listed in this subsection amount to full description of the ac-driven dynamics of an isolated TLS. In the next Section, we will briefly outline several applications of our theory. For simplicity, we will mostly focus on the properties of the non-dissipative dynamics.

IV. EXPERIMENTAL MANIFESTATIONS

In this Section we discuss the physical behavior of several quantities which can be probed experimentally for various physical realizations of the TLS. Before we proceed with the discussion on the application of our results and computation of physical observables, we derive the expression for the evolution operator and the density matrix which will allow us to compute probabilities which characterize the dynamics of the TLS.

Evolution operator $\hat{S}(t)$ is defined by

$$\Psi_g(t) = \hat{S}(t) \Psi_g(0). \quad (38)$$

From expressions (35) one can always write down a general expression for the evolution operator, which is valid for arbitrary initial conditions:

$$\hat{S}(t) = \begin{pmatrix} \psi_+(t) & \psi_-^*(t) \\ \psi_-(t) & -\psi_+^*(t) \end{pmatrix} \begin{pmatrix} \psi_+^*(0) & \psi_-^*(0) \\ \psi_-(0) & -\psi_+(0) \end{pmatrix} \quad (39)$$

Note that it is now straightforward to derive the density matrix from (39) using the following expression:²⁷

$$\hat{\rho}(t) = \hat{S}(t)\hat{\rho}_0\hat{S}^\dagger(t), \quad (40)$$

where $\hat{\rho}_0$ is the density matrix of an initial state of the TLS. The expressions (39,40) can be used as a basis to analyze the effects of the environment dissipation on the dynamics of the TLS. In particular, one can determine the probability of the TLS to remain in the initially prepared state $P_{\uparrow\rightarrow\uparrow}(t)$.

A. Coherent destruction of tunneling

The phenomenon of the coherent destruction of tunneling (CDT) has been predicted theoretically^{28–30} for various physical realizations. Qualitatively, this phenomenon can be interpreted as the dynamical trapping of the TLS in one its states. For example, CDT occurs when the survival probability of the initial state dynamically approaches unity. This phenomenon has its counterpart known in literature as driving induced tunneling oscillations. This effect has been first analyzed theoretically in a series of papers^{31–33} and observed experimentally for the first time by Nakamura *et al.*³⁴ To compute the sur-

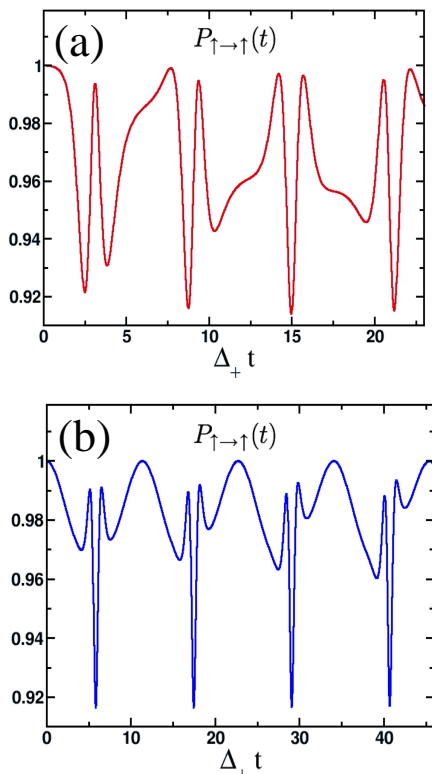


FIG. 6: Plots of the return probability $P_{\uparrow\rightarrow\uparrow}(t)$, Eq (41), in the limit of the strong ac-driving: (a) $\varepsilon = 8.5\Delta_t$, $\mathcal{A}_f = 13.5\Delta_t$, $\omega_f = 21\Delta_t$; (b) $\varepsilon = 0.1\Delta_t$, $\mathcal{A}_f = 13.5\Delta_t$, $\omega_f = 8\Delta_t$.

vival probability $P_{\uparrow\rightarrow\uparrow}(t)$ we can use the density matrix

(40). It is, however, easier to use an expression for the wave function (35) with the initial conditions (36,37). In particular, let us choose the initial amplitudes such that both C_1 and C_2 are real and introduce an angle ϑ , so that $C_1 = \cos(\vartheta/2)$.

After some algebra, we obtain the following expression for the return probability

$$P_{\uparrow\rightarrow\uparrow}(t) = \frac{1}{2} + \cos\vartheta \cdot m_z(t) + \sin\vartheta \cos[2\alpha(t)] \cdot \sqrt{\frac{1}{4} - m_z^2(t)}. \quad (41)$$

The CDT occurs when $P_{\uparrow\rightarrow\uparrow}(t) \approx 1$ and we assume the initial conditions (36). From (41) it follows that if we perform an averaging over time frame longer than T_f and $T_h = 2\pi/\nu$, the third term in (41) averages out to zero, so that employing (14) we find

$$\langle P_{\uparrow\rightarrow\uparrow}(t) \rangle \simeq \frac{1}{2} + 2 \cos\vartheta \Delta_t B \left(\varepsilon - \frac{c_1}{\Delta_t^2} \right). \quad (42)$$

This equation approximately determines the parameter range for which CDT occurs. Fig. 5 displays representative results for the return probability and illustrates the CDT phenomenon: As we can see, in the limit of strong driving, i.e. when $\mathcal{A}_f \gg \Delta_t$ and $\omega_f \gg \Delta_t$, the return probability remains of order unity, which implies that the tunneling processes become strongly suppressed. We also have found that CDT remains robust and is present as long as the parameters Δ_a and Δ_\pm are such that the dynamics of the TLSs remains in the strong driving regime. This qualitative behaviour of tunneling was found to be essentially independent of the ratio ε/Δ_t . These our findings agree qualitatively with the results reported previously in Ref. [15] for the monochromatic AC-field. Finally, we note that if a system of charged TLSs, e.g. OH-rotors present in Al_2O_3 dielectrics, is driven into such non-linear CDT regime by an external AC electric field, then the TLS tunneling and the corresponding dipole polarization dynamics will be strongly reduced. This suggest that a strong non-linear drive may actually correspond to lower losses.

B. Dielectric response

Fig. 1 provides a pictorial example of a TLS charged defect, – an OH-rotor, which is one of the most likely candidates of physical two-level-systems responsible for dielectric losses in superconducting qubits. This rotor has a non-zero dipole moment \vec{p} and, therefore, responds to an applied external electric field $\vec{\mathcal{E}}(t)$. In the absence of other interactions which may affect TLS dynamics, the Hamiltonian describing the dynamics is (10) with $f(t) = \varepsilon + \vec{p} \cdot \vec{\mathcal{E}}(t)$. By construction, the average dipole moment of an isolated TLS is determined by the following average within the spin mapping⁵

$$\vec{d}(t) = m_z(t)\vec{p}. \quad (43)$$

The linear dielectric response function can be computed from (43) by differentiating the corresponding components of the average dipole moment with respect to the amplitude of an external field $\vec{\mathcal{E}}$. To define a non-linear dielectric response function corresponding to a solution $m_z(t)$, which generally is a complicated function of the amplitude, we consider the spin-spin correlation function. Up to a pre-factor, given by the angle between the initial direction of the dipole moment relative to the external electric field, the dielectric response of an isolated TLS is defined by the Fourier component of the following correlator⁵

$$\epsilon(\omega) = \frac{i}{4} \int_0^{\infty} e^{i\omega t} e^{-t/\tau} \langle [\hat{\sigma}_z(t), \hat{\sigma}_z(0)] \rangle dt \quad (44)$$

where square brackets denote a commutator between the corresponding spin operators. The exponential prefactor describes the dissipative effects of the environment and averaging is taken over the initial state of the TLS. We are introducing the dissipative effects on a phenomenological level only and ignore the difference between the relaxation and dephasing processes. This is sufficient to get insight into the general properties of the exact spectrum of the dielectric response due to an ensemble of identical TLS. Operators $\hat{\sigma}_\alpha(t)$ in Eq. (44) correspond to the Heisenberg representation:

$$\hat{\sigma}_z(t) = \hat{S}^\dagger(t) \hat{\sigma}_z \hat{S}(t). \quad (45)$$

We remind the reader that formally the evolution operator $\hat{S}(t)$ is given by

$$\hat{S}(t) = \hat{T} \exp \left[-i \int_0^t H(t') dt' \right], \quad (46)$$

with \hat{T} being a time-ordering operator. Using (39) and assuming the initial conditions $\Psi^\dagger(0) = (a^*, b^*)$, for the correlator $\mathcal{K}(t) = \frac{i}{4} \langle [\hat{\sigma}_z(t), \hat{\sigma}_z(0)] \rangle$ under the integral in (44) we find:

$$\mathcal{K}(t) = 4(|a|^2 - |b|^2) m_\perp(t) \sin[2\alpha(t)] + 8i \text{Im}[a^* b] \times \{ m_z(0) m_x(t) - m_x(0) m_\perp(t) \cos[2\alpha(t)] \}. \quad (47)$$

Here $m_\perp(t) = \sqrt{1/4 - m_x^2(t)}$ and we have fixed the initial value of the field so that $\dot{f}(0) = 0$. The subsequent time integration yields an expression for the dielectric response function. Analytic analysis of the response function $\epsilon(\omega)$ is hindered by the fact that the correlation function $\mathcal{K}(t)$ is only a quasi-periodic function of time, since it is expressed as a combination of two periodic functions with different periods T_f and T_h (33), so that we have to resort to numerical calculation. In Fig. 6, we present representative plots of the real and imaginary part of $\epsilon(\omega)$ (44) for the initial conditions (36). To interpret our results, we recall that the common phase, $\alpha(t)$, can be written as a sum of a linear-in- t term plus a periodic

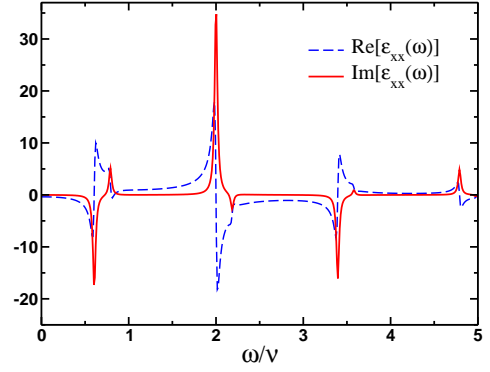


FIG. 7: Plot of real and imaginary part of the response function $\epsilon(\omega)$. Note that discontinuities in real part and the peaks in imaginary part of the response function appear at frequencies $\omega_{dis} = 2(n\omega \pm \nu)$, ($n = 0, \pm 1, \pm 2, \dots$) in agreement with expression (48). These plots have been obtained for the following values of the parameters: $\Delta_a = 0.15\Delta_+$, $\Delta_- = 0.3\Delta_+$ and $\Delta_t = 0.5\Delta_+$.

function (33). Since $m_\perp(t)$ is a periodic function with the period T_f , we can express the corresponding terms in (47) in a Fourier series. Subsequent time integration yields a response function of the following type:

$$\epsilon(\omega) = \sum_{n=-\infty}^{\infty} \frac{\chi_n}{\omega - 2n\omega_f \pm 2\nu + \frac{i}{\tau}}, \quad (48)$$

where ϵ_n are the corresponding Fourier coefficients. From this expression, we see that the peaks in the imaginary part of the response function describing the energy losses due to TLSs appear at frequencies, $\omega_{dis} = 2(n\omega \pm \nu)$, commensurate with the driving frequency but with an overall shift determined by the quantum mechanical phase collected by a TLS over one cycle, ν . Note that within the linear response theory, one typically keeps only the lowest Fourier harmonic in the spectrum ($n = 0$) and neglects all others. For the case of a monochromatic field the Fourier component with $n = 0$ is kept so that

$$\epsilon_{lin}(\omega) = \epsilon_0 \sum_{a=\pm} \frac{1}{\omega + 2a\nu + \frac{i}{\tau}}, \quad (49)$$

and we recover the textbook result for the dielectric response function.⁵ For a fixed set of parameters, however, one would only keep the largest contribution to the imaginary part of $\epsilon(\omega)$. For example, the imaginary part of $\epsilon(\omega)$ is the largest for $\omega^* \simeq 2\nu$. Note also that apart from a difference in the value of the resonant frequency (which in the regime of weak driving is given by the energy that governs a stationary time evolution of a TLS eigenstate in the absence of any perturbations, $\nu = \sqrt{\Delta_t^2 + \varepsilon^2}$, the response functions for the case of monochromatic field and the field given by (23) are qualitatively the same.

In the array of non-interacting TLS, the response function must be averaged over a distribution of the barrier

heights, direction of the electric field etc. We leave the detailed analysis directly applicable to the array of non-interacting and pairwise interacting TLS for a future publication.

V. CONCLUSIONS

In this paper we presented an exact solution for the problem of AC-driven dynamics of a generic two-level system. Our approach was based on constructing a nonlinear differential equation for the driving field, which has admitted an exact solution. The key feature of our solution for the external field is that it is fully described by three independent parameters. We have shown that one can interpret different nonlinear combinations of these parameters as an amplitude, frequency and a DC-component of the field. Being very general in nature, we believe that our results and methods can be applied to a wide variety of experiments ranging from NMR to the analysis of dielectric losses in amorphous materials.

This research was supported by the Intelligence Advanced Research Projects Activity (IARPA) through the US Army Research Office award W911NF-09-1-0351. Authors would like to thank Slava Dobrovitski and Roman Lutchyn for discussions related to this work.

Appendix A: calculation of the parameters e_j

In this Appendix, we provide explicit expressions for the parameters e_j 's, which determine the explicit form of our exact solution for the external field (22). As mentioned in the main text, the particular expressions for these parameters, e_j , depend on the relative values of Δ_a and Δ_{\pm} . For the choice corresponding to

$$\Delta_a \geq \frac{\Delta_- + \Delta_+}{2}, \quad (\text{A1})$$

we have

$$\begin{aligned} e_1^{(1)} &= \frac{1}{3}(2 - a_+ - a_-), \\ e_2^{(1)} &= \frac{1}{3}(2a_- - a_+ - 1), \\ e_3^{(1)} &= \frac{1}{3}(2a_+ - a_- - 1). \end{aligned} \quad (\text{A2})$$

In the opposite case of

$$\frac{\Delta_+ - \Delta_-}{2} \leq \Delta_a \leq \frac{\Delta_- + \Delta_+}{2}, \quad (\text{A3})$$

we have

$$\begin{aligned} e_1^{(2)} &= \frac{1}{3}(2a_- - a_+ - 1), \\ e_2^{(2)} &= \frac{1}{3}(2 - a_- - a_+), \\ e_3^{(2)} &= \frac{1}{3}(2a_+ - a_- - 1). \end{aligned} \quad (\text{A4})$$

Finally when

$$\Delta_a \leq \frac{\Delta_+ - \Delta_-}{2}, \quad (\text{A5})$$

we have

$$\begin{aligned} e_1^{(3)} &= \frac{1}{3}(2a_- - a_+ - 1), \\ e_2^{(3)} &= \frac{1}{3}(2a_+ - a_- - 1), \\ e_3^{(3)} &= \frac{1}{3}(2 - a_- - a_+). \end{aligned} \quad (\text{A6})$$

We also remind the reader, that the coefficients a_{\pm} in the above equations are given by $a_{\pm} = 2\Delta_{\pm}/(\Delta_+ + 2\Delta_a \pm \Delta_-)$.

Appendix B: Exact solution for the function $f(t)$: special cases

In this Appendix, we consider a few special cases, where the exact solution given by (23) (which is generally described by three independent parameters) is reduced to a degenerate function with simpler properties, which is characterized by two parameters only. The first case we consider corresponds to $\Delta_a \rightarrow 0$. As shown below, the choice of $\Delta_- \simeq \Delta_+$, corresponds to an external field of the following form, $f(t) \simeq \Delta_+[1 + q \cos(2\Delta_+ t)]$ with $q \ll 1$. Another case considered here is the limit $\Delta_- \rightarrow 0$, but with both Δ_a and Δ_+ kept finite. In that case, $f(t)$ can be represented as a single isolated soliton.

1. Limit of $\Delta_a \rightarrow 0$

Our goal here is to recover the limiting case for our solution corresponding to $\delta_a = 0$. It can be shown that in this limit,

$$\kappa = \frac{1 - k'}{1 + k'}, \quad k' = \delta_-, \quad k = \sqrt{1 - k'^2} \quad (\text{B1})$$

and the solution for the driving field reads:

$$f(t) = \Delta_+ \left\{ \frac{2}{\mathcal{P}[k\Delta_+(t - t_0)] + 1 - e_3} - 1 \right\}. \quad (\text{B2})$$

We demonstrate below that the expression in the brackets can be cast into single Jacobi elliptic function $\text{dn}(\Delta_+ t, k)$. For this, we use the identity

$$\mathcal{P}\left(\frac{u}{\sqrt{e_1 - e_3}}\right) = e_3 + (e_1 - e_3) \frac{1}{\text{sn}^2(u, \kappa)}, \quad (\text{B3})$$

such that it gives

$$f(t) = \Delta_+ \left[\frac{\text{sn}^2(u, \kappa) - (e_1 - e_3)}{\text{sn}^2(u, \kappa) + (e_1 - e_3)} \right] \quad (\text{B4})$$

and variable u equals $u = \frac{1}{2}(1 + \delta_-)\Delta_+ t$. This expression can be further simplified by means of the following relation between the Jacobi elliptic functions:

$$\operatorname{dn}(u_1, \kappa_1) = \frac{1 - \kappa \operatorname{sn}^2(u, \kappa)}{1 + \kappa \operatorname{sn}^2(u, \kappa)}, \quad (\text{B5})$$

where

$$u_1 = (1 + \kappa)u, \quad \kappa_1 = \frac{2\sqrt{\kappa}}{1 + \kappa} \quad (\text{B6})$$

Indeed, from expressions (A6) for $\Delta_a = 0$ we have

$$\kappa = \sqrt{\frac{e_2 - e_3}{e_1 - e_3}} = \frac{1 - \delta_-}{1 + \delta_-} = \frac{1}{e_1 - e_3}, \quad (\text{B7})$$

so that $\kappa_1 = k$ and we find:

$$f(t) = -\Delta_+ \operatorname{dn}[\Delta_+(t - t_0), k]. \quad (\text{B8})$$

Finally, when $k \rightarrow 0$ ($\Delta_- \rightarrow \Delta_+$) it follows²⁶ that

$$f(t) \simeq -\Delta_+ [1 + q \cos(2\Delta_+ t)], \quad q \ll 1, \quad (\text{B9})$$

We find that for the special values of parameters the line shape of the external field is given by the cosine.

2. Limit $\Delta_- \rightarrow 0$

To derive an explicit form of the driving field, $f(t)$, in this case, we work with the general solution (23). Let us first assume that

$$\Delta_a \leq \Delta_+/2.$$

Then, the case $\Delta_- = 0$ corresponds to $k = 1$, which in turn implies

$$\operatorname{sn}(u, 1) = \tanh(u), \quad u = \frac{1}{2}\lambda t \quad (\text{B10})$$

and $\lambda = \sqrt{\Delta_+^2 - 4\Delta_a^2}$. After some simple algebra, we find

$$f = - \left[\Delta_a + \frac{\lambda^2}{2\Delta_a - \Delta_+ \cosh(\lambda t)} \right], \quad (\text{B11})$$

which up to the minus sign, is exactly the same expression as the listed in Ref. [25]. Finally, let us consider the parameter range with

$$\Delta_a \geq \Delta_+/2. \quad (\text{B12})$$

According to the expressions above for that case $k = 0$ and $\operatorname{sn}(u, 0) = \sin(\sqrt{4\Delta_a^2 - \Delta_+^2}t/2)$. It follows:

$$f = -\Delta_a + \frac{4\Delta_+(2\Delta_a - \Delta_+)/ (2\Delta_a + \Delta_+)}{1 - \cos\left(\sqrt{4\Delta_a^2 - \Delta_+^2}t\right) + 2\frac{2\Delta_a - \Delta_+}{2\Delta_a + \Delta_+}}. \quad (\text{B13})$$

We see that when $\Delta_- = 0$ external field has a line shape of a single pulse. Note that our solutions (B11,B13) do not contradict to our assumption of the periodicity of $f(t)$ since both these solutions correspond to the case where the period of $f(t)$ goes to infinity.

Appendix C: calculation of the common phase $\alpha(t)$

In this Appendix, we outline the main steps, which allow to compute the integral (32) exactly. The calculation includes the following transform of the special functions involved that reduces the integrand to a form amenable for exact integration of the Weierstrass elliptic function:²⁶

$$\int \frac{\alpha \mathcal{P}(u) + \beta}{\gamma \mathcal{P}(u) + \delta} du = \frac{\alpha}{\gamma} u + \frac{\alpha\delta - \beta\gamma}{\gamma\delta} \times \left[\log \frac{\sigma(u+v)}{\sigma(u-v)} - 2u\zeta(v) \right], \quad (\text{C1})$$

where $\alpha, \beta, \gamma, \delta$ are some constants, a parameter v is determined from the derivative of the Weierstrass function, $\mathcal{P}'(v) = -\delta/\gamma$, $\sigma(u)$, and $\zeta(u)$ are the Weierstrass elliptic sigma and zeta functions.²⁶

The next step is to write down the function, $f(t)$, explicitly in terms of the Weierstrass function. Combining expressions (18,20,22), we have:

$$f(t) = -\Delta_+ \left[\frac{\mathcal{P}(x + \omega') - 1 - e_j}{\mathcal{P}(x + \omega') + 1 - e_j} \right] - \Delta_a \quad (\text{C2})$$

where $a_{\pm} = 2\Delta_+ / (\Delta_+ + 2\Delta_a \pm \Delta_-)$, $x = \frac{\Delta_+ t}{\sqrt{a_+ a_-}}$ and $j = 1, 2$ or 3 depending on the value of Δ_a (see Appendix A). Let us now consider the first integral in (32):

$$\int_0^t \frac{d_+^2}{f^2(t') - d_+^2} dt' = \frac{\sqrt{a_+ a_-}}{2\Delta_+} \int_0^x \left\{ \frac{d_+ [\mathcal{P}(x' + \omega') + 1 - e_j]}{(\Delta_+ + \Delta_a - d_+) \mathcal{P}(x' + \omega') + (\Delta_a - d_+)(1 - e_j) - \Delta_+(1 + e_j)} - (d_+ \rightarrow -d_+) \right\} dx' \quad (\text{C3})$$

Here the index j of the coefficient e_j is determined by the value of Δ_a (see Appendix A). The remaining terms can be written in a similar form and the corresponding integrals can be evaluated using (C1), as we have done

for the first one (C3). Since the resulting expressions for the $\alpha(t)$ turn out to be too cumbersome, we do not list them here.

-
- ¹ U. Weiss, *Quantum dissipative systems* (Wold Scientific, Singapore, 2008), 3rd Ed.
 - ² A. J. Leggett *et al.*, Rev. Mod. Phys. **59**, 1 (1987).
 - ³ P. W. Anderson, B. Halperin and C. Varma, Phil. Mag. **25**, 1 (1972).
 - ⁴ C. C. Yu and P. W. Anderson, Phys. Rev. B **29**, 6165 (1984).
 - ⁵ S. Hunklinger and A. K. Raychaudhuri, *Amorphous Solids: Low-Temperature Properties*, edited by W. A. Phillips (Springer, Berlin, 1981).
 - ⁶ V. Lubchenko and P. G. Wolynes, J. Chem. Phys. **119** (17) 9088 (2002).
 - ⁷ M. A. Nielsen, I. L. Chuang, *Quantum Computations and Quantum Information* (Cambridge Univ. Press, Cambridge, 2002).
 - ⁸ B. D. Gerardot and P. Öhberg, Science **326**, 1489 (2009).
 - ⁹ J. E. Mooij, T. P. Orlando, L. Levitov, L. Tian, C. H. van der Wal, and S. Lloyd, Science **285**, 1036 (1999).
 - ¹⁰ C. H. van der Wal, A. C. J. ter Haar, F. K. Wilhelm, R. N. Schouten, C. J. P. M. Harmans, T. P. Orlando, S. Lloyd, and J. E. Mooij, Science **290**, 773 (2000).
 - ¹¹ I. Chiorescu, Y. Nakamura, C. J. P. M. Harmans, and J. E. Mooij, Science **299**, 1869 (2003).
 - ¹² G. D. Fuchs *et al.*, Science **326**, 1520 (2009).
 - ¹³ J. M. Martinis *et al.*, Phys. Rev. Lett. **95**, 210503 (2005).
 - ¹⁴ H. Wang *et al.*, *pre-print* arXiv:0909.0547 [cond-mat.mesh-hall] (2009).
 - ¹⁵ J. Hausinger and M. Grifoni, *pre-print* arXiv:0910.0356 [quant-ph] (2009).
 - ¹⁶ W. A. Phillips, J. of Low Temp. Phys. **11**, 757 (1973).
 - ¹⁷ C. Musgrave, *private communication*.
 - ¹⁸ H. Paik and K. D. Osborn, Appl. Phys. Lett. **96**, 072505 (2010).
 - ¹⁹ R. A. Barankov, L. S. Levitov, and B. Z. Spivak: Phys. Rev. Lett. **93**, 160401 (2004); R. A. Barankov and L. S. Levitov, Phys. Rev. Lett. **96**, 230403 (2006).
 - ²⁰ E. A. Yuzbashyan, B. L. Altshuler, V. B. Kuznetsov, V. Z. Enolskii: J. Phys. A **38**, 7831 (2005); E. A. Yuzbashyan, B. L. Altshuler, and V. B. Kuznetsov: Phys. Rev. B **72**, 144524 (2005); E. A. Yuzbashyan, B. L. Altshuler, V. B. Kuznetsov, V. Z. Enolskii: Phys. Rev. B **72**, 220503 (2005); E. A. Yuzbashyan and M. Dzero, Phys. Rev. Lett. **96**, 230404 (2006).
 - ²¹ E. A. Yuzbashyan, O. Tsypliyatyev and B. L. Altshuler, Phys. Rev. Lett. **96**, 097005 (2006).
 - ²² P. W. Anderson, Phys. Rev. **112**, 1900 (1958).
 - ²³ V. M. Galitski, arXiv:1003.2237v1 (2010).
 - ²⁴ M. Dzero, E. A. Yuzbashyan, B. L. Altshuler and P. Coleman, Phys. Rev. Lett. **99**, 160402 (2007).
 - ²⁵ E. A. Yuzbashyan, Phys. Rev. B **78**, 184507 (2008).
 - ²⁶ I. S. Gradstein and I. M. Ryzhik, *Tables of Integrals, Series, and Products* (Academic Press, San Diego, 1994).
 - ²⁷ R. P. Feynman, *Statistical Mechanics: A Set of Lectures* (Addison-Wesley, New York, 1972).
 - ²⁸ F. Grossmann, T. Dittrich, P. Jung, and P. Hänggi, Phys. Rev. Lett. **67**, 516 (1991).
 - ²⁹ F. Grossmann, P. Jung, T. Dittrich, and P. Hänggi, Z. Phys. B **84**, 315 (1991).
 - ³⁰ F. Grossmann and P. Hänggi, Europhys. Lett. **18**, 571 (1992).
 - ³¹ L. Hartmann, M. Grifoni, and P. Hänggi, J. Chem. Phys. **109**, 2635 (1998).
 - ³² L. Hartmann, I. Goychuk, M. Grifoni, and P. Hänggi, Phys. Rev. E **61**, R4687 (2000).
 - ³³ I. Goychuk and P. Hänggi, Adv. Phys. **54**, 525 (2005).
 - ³⁴ Y. Nakamura, Y. A. Pashkin, and J. S. Tsai, Phys. Rev. Lett. **87**, 246601 (2001).